Direct AC/DC Rectifier with Mitigated Low-Frequency Ripple Through Waveform Control

Sinan Li[1], Guorong Zhu[2], Siew-Chong Tan[1], S.Y.R. Hui[1]
[1]Department of Electrical & Electronic Engineering, The University of Hong Kong, Hong Kong, China
[2]School of Automation, Wuhan University of Technology, Wuhan, China

Abstract— **In a rectification system with unity power factor, the input power consists of a DC and a double-line frequency power component. Traditionally, an electrolytic capacitor (E-Cap) is used to buffer the double-line frequency power such that the DC output presents a small voltage ripple. The use of E-Cap significantly limits the lifetime of the rectifier system. In this paper, a differential AC/DC rectifier based on the use of an inductor-current waveform control methodology is proposed. The proposed configuration achieves single-stage direct AC/DC rectification without the needs of a front-stage diode rectifier circuit, an input EMI filter, and an E-Cap for buffering the double-line frequency power. The feasibility of the proposal has been practically confirmed in an experimental prototype.**

I. INTRODUCTION

Unity power factor, high efficiency, high reliability, compact size, and low cost are the typical desired features of conventional AC/DC rectification systems. With the anticipated increasing adoption of light-emitting-diode (LED) lighting, new requirements are expected of the rectification systems. Important criteria like achieving (1) reduced flickering of lighting systems by reducing DC side low-frequency current ripple and (2) longer system lifetime and enhanced reliability should be taken into the system's design consideration. The reason for the former criteria is that in typical 50 Hz or 60 Hz single-phase rectification systems, the low-frequency rectified current ripple is 100 Hz or 120 Hz, respectively [1]. For LED lighting, a large low-frequency current variation would imply noticeable flickering, which can also shorten the lifetime of LEDs [2]–[7]. For the latter criteria on achieving longer system lifetime and enhanced reliability, the objective is to ensure that LED ballasts are of compatible lifetime with that of the LED, which is up to 100,000 hours [8]. For EV applications, low-frequency variations are detrimental to the storage properties of the battery banks, which are the critical components of an EV's electrical system [9]. Generally speaking, the electrolytic capacitors (E-cap) adopted in the ballasts and other rectification systems have been recognized as weak point in the overall system's reliability. It is worthy to consider converter topologies that do not mandate the use of E-cap in rectification systems so as to achieve long lifetime and high reliability and at the same time maintain minimal low-frequency ripple at its DC output. Recently, many research efforts have been devoted to develop AC-DC power converter topologies without using E-caps [2]–[7], [9]–[15]. Both active [2]–[7], [9]–[13] and passive [14], [15] approaches have been reported in recent literature.

In this paper, a direct (electrolytic-capacitor-free) AC/DC rectifier with mitigated low-frequency ripple through the use of inductor-current waveform control is proposed. The proposed system allows the use of differential topologies to directly rectify power from the AC source to the DC load (i.e. a single-stage AC/DC rectification) without needing the front-stage diode rectifier circuit. Other than the merit of automatically achieving high power factor correction, an added feature of this system is that the conducted EMI at front-end is automatically alleviated without the need for a large EMI filter.

II. PROPOSED DIRECT AC/DC DIFFERENTIAL RECTIFIER SYSTEM

Fig. 1(a) shows the general concept of the direct AC/DC differential rectification system, in which two bidirectional DC/DC converters are connected in a series-input and parallel-output configuration. Here, v_{c1} and v_{c2} are respectively the input voltage of each of the two converters, whereby v_{c1} and v_{c2} are in opposing polarity and their difference is a pure sinusoidal waveform that follows the shape of the input AC source v_{ac}. Noteworthy is that the bidirectional DC/DC converters adopted in this configuration can be of any type, and the design choice will be based on the requirements for stepping up or down the output voltage, isolation, input/output EMI filter requirement etc., as required in typical DC/DC power converter designs. Fig. 1(b) shows a buck differential rectifier (case-study example used in this paper), which comprises two bidirectional buck converters connected under the proposed configuration [16].

The main features of the proposed differential rectifier system are that it can

- inherently achieve single-stage rectification without the need for front-stage diode rectifier;
- inherently realize PFC function;
- facilitate the use of the waveform control technique proposed in [1], which allows the system to

This work was supported by Hong Kong Research Grant Council under the Theme-based Research Project: T22-715/12-N.

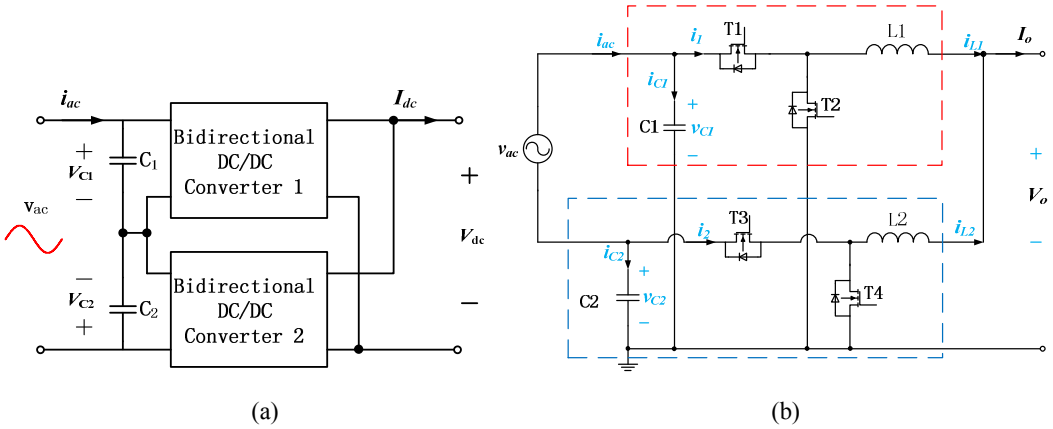

Fig. 1. (a) Conceptual diagram of the proposed differential rectifier and (b) a buck differential rectifier.

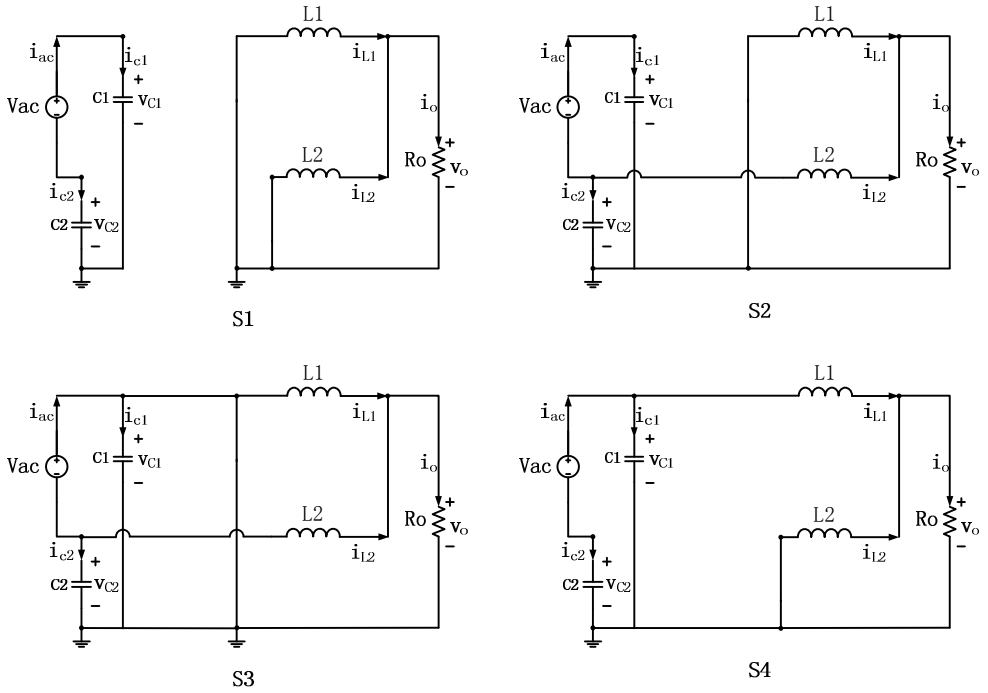

Fig. 2. Equivalent circuits of the buck differential rectifier in various operating states.

concurrently achieve good-quality single-stage AC/DC rectification and second-harmonic-ripple-free DC/DC conversion without the use of electrolytic capacitor.

The capacitor-voltage waveform control method is originally proposed for differential inverters [1], the control of which involves only the regulator for the AC side capacitor voltages v_{c1} and v_{c2}. In the case of the differential rectifier, a different set of control variables and a different controller are needed.

Table I shows the four possible operating states S_1, S_2, S_3, and S_4 of the buck differential rectifier in a complete line cycle with respect to the on/off states of the switches $T_1 - T_4$. The corresponding equivalent circuits are given in Fig. 2. In the positive half of the line cycle, the possible states are S_1, S_2, and S_3, and in the negative half of the line cycle, the possible states are S_1, S_3, and S_4. All possible operating conditions for switches T_1 and T_3 during the positive and negative half line cycles are depicted in Fig. 3 and Fig. 4.The duty cycles for the rectifier must satisfy (1) such that d_{low} (duty ratio of the low-side converter with respect to T_3) is always larger than or

equal to d_{high} (duty ratio of the high-side converter with respect to T_1) during positive line cycle, and vice versa. Here, only the positive half line cycle is examined since the operation is symmetrical between the positive and negative half of the line cycle.

TABLE I. OPERATING STATES OF BUCK DIFFERENTIAL RECTIFIER

Switch / State	T_1 (high side)	T_2 (high side)	T_3 (low side)	T_4 (low side)
S_1	OFF	ON	OFF	ON
S_2	OFF	ON	ON	OFF
S_3	ON	OFF	ON	OFF
S_4	ON	OFF	OFF	ON

$$\begin{cases} v_{ac} > 0 \Rightarrow d_{low} > d_{high} \\ v_{ac} < 0 \Rightarrow d_{low} < d_{high} \\ v_{ac} = 0 \Rightarrow d_{low} = d_{high} \end{cases} \quad (1)$$

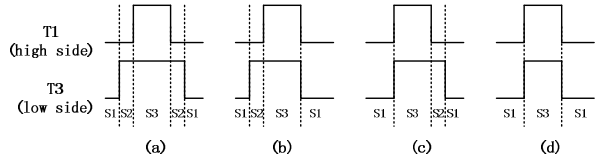

Fig. 3. Possible operation conditions during positive half line cycle.

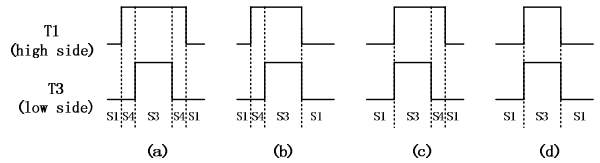

Fig. 4. Possible operation conditions during negative half line cycle.

By setting d_1, d_2, d_3, and d_4 as the ratios of the respective time interval of each state $S_1 - S_4$ shown in Fig. 3 over one switching period, d_{low} and d_{high} can be expressed as

$$d_{low} = d_2 + d_3 \quad (2)$$

$$d_{high} = d_3 \quad (3)$$

By using state-space average modeling,

$$\begin{cases} V_{C1} = \dfrac{D_2 + D_3}{D_2} V_{ac} = \dfrac{D_{low}}{D_{low} - D_{high}} V_{ac} \\ V_{C2} = \dfrac{D_3}{D_2} V_{ac} = \dfrac{D_{high}}{D_{low} - D_{high}} V_{ac} \\ I_{L1} = \dfrac{1}{D_3}(I_{ac} - I_{C1}) = \dfrac{1}{D_{high}} I_1 \\ I_{L2} = \dfrac{1}{D_2 + D_3}(I_{ac} + I_{C1}) = \dfrac{1}{D_{low}} I_2 \end{cases} \quad (4)$$

where I_{L1}, I_{L2}, V_{C1}, V_{C2}, D_2, D_3, D_{low} and D_{high}, are the steady-state values of i_{L1}, i_{L2}, v_{C1}, v_{C1} , d_2, d_3, d_{low} and d_{high}.

From (4), the average output current and voltage of the rectifier can be resolved as

$$\begin{cases} I_o = I_{L1} + I_{L2} = \dfrac{1}{D_{high}} I_1 - \dfrac{1}{D_{low}} I_2 \\ V_o = (I_{L1} + I_{L2}) R_o = (\dfrac{1}{D_{high}} I_1 - \dfrac{1}{D_{low}} I_2) R_o \end{cases} \quad (5)$$

where R_o is the DC side loading.

It is found from (4) that V_{C1} and V_{C2} are coupled functions of D_{low} and D_{high}. Therefore, if V_{C1} and V_{C2} are chosen as the control variables, the control is not straightforward since it involves the operation of both converters simultaneously. Here, the D_{low} and D_{high} cannot be resolved explicitly with respect to V_{C1}, V_{C2} and V_{ac}.

On the other hand, inductor currents I_{L1} and I_{L2} are decoupled between the two converters and are independent functions of D_{low} and D_{high}, as can be seen in (4). The duty cycles of the two converters can be easily resolved as

$$\begin{cases} D_{low} = \dfrac{I_2}{I_{L2}} \\ D_{high} = \dfrac{I_1}{I_{L1}} \end{cases} \quad (6)$$

Therefore, by choosing I_{L1} and I_{L2} as control variables for the buck differential rectifier, the control becomes simple and straightforward as compared with capacitor-voltage waveform control [1] because the two current variables are not mutually coupled.

III. Application of General Waveform Control Method To The Proposed Differential Rectifier

In conventional rectifier systems with unity power factor, a DC-link electrolytic capacitor is typically required to buffer

the second-harmonic power pulsation between the AC input and the DC output. This capacitor is known to be a critical source of system failure. For the proposed differential rectifier system, a general waveform control technique is implemented to mitigate the second-harmonic power pulsation between the AC input and the DC output, without the use of a DC-link electrolytic capacitor. This method is evolved from the work described in [1], which is originally developed for the full-bridge (boost-type differential) inverters. The waveform control method described here is general and applicable to any differential rectifier systems.

Traditionally, without waveform control, the two capacitor voltages are in the form of

$$v_{c1} = V_d + 0.5V_{\max}\sin(\omega t) \tag{7}$$

$$v_{c2} = V_d - 0.5V_{\max}\sin(\omega t) \tag{8}$$

Due to the differential connection of C_1 and C_2, their differential voltage is equal to the AC line voltage, i.e.,

$$v_{ac} = v_{c1} - v_{c2} = V_{\max}\sin(\omega t) \tag{9}$$

The DC output i_o will inevitably contain a significant level of double-line frequency current ripple $i_{o(2\omega)}$ as given in

$$i_o = I_o + i_{o(2\omega)} \tag{10}$$

It is demonstrated in [20] that, given the operation waveforms described in (7) and (8), the two capacitors C_1 and C_2 do not contribute to the absorption of the double-line frequency power from the AC input, but serve only as high frequency filters. By introducing a double-line frequency component to control v_{C1} and v_{C2}, C_1 and C_2 are able to storage the double-line pulsation power as well, thereby mitigating the double-line frequency ripple at the DC output.

Assuming that the input capacitor voltages are in the form

$$v_{c1} = V_d + kV_{\max}\sin(\omega t) + B\sin(2\omega t + \varphi) \tag{11}$$

$$v_{c2} = V_d + (k-1)V_{\max}\sin(\omega t) + B\sin(2\omega t + \varphi) \tag{12}$$

where k is the ratio of the amplitude of the line-frequency component for the high-side converter against the amplitude of the line voltage $V_{\max}$, and B is the amplitude of the double-line frequency component. Both v_{c1} and v_{c2} contain a DC, a fundamental, and a second-harmonic component. Due to the differential connection of C_1 and C_2, their differential voltage is equal to the AC input source, i.e.,

$$v_{ac} = v_{c1} - v_{c2} = V_{\max}\sin(\omega t) \tag{13}$$

The current flow into C_1 and C_2 can be derived respectively as

$$i_{c1} = C_1\frac{dv_{c1}}{dt} = kC_1\omega V_{\max}\cos(\omega t) + 2\omega C_1 B\cos(2\omega t + \varphi) \tag{14}$$

$$i_{c2} = C_2\frac{dv_{c2}}{dt} = (k-1)C_2\omega V_{\max}\cos(\omega t) + 2\omega C_2 B\cos(2\omega t + \varphi) \tag{15}$$

The average input current of each converter in the rectifier can be derived as

$$i_1 = i_{ac} - i_{c1} = I_{\max}\sin(\omega t) - kC_1\omega V_{\max}\cos(\omega t) - 2\omega C_1 B\cos(2\omega t + \varphi) \tag{16}$$

$$i_2 = -i_{ac} - i_{c2} = -I_{\max}\sin(\omega t) - (k-1)C_2\omega V_{\max}\cos(\omega t) - 2\omega C_2 B\cos(2\omega t + \varphi) \tag{17}$$

where I_{max} is the peak amplitude of the line current.

Assuming the converters to be lossless, the input power equals the output power, of which the inductor currents can be derived as

$$i_{L1} = \frac{i_1 \times v_{c1}}{V_o} = \frac{i_1}{d_{high}} \quad \text{and} \quad i_{L2} = \frac{i_2 \times v_{c2}}{V_o} = \frac{i_1}{d_{low}} \tag{18}$$

The total output current is thereby given as

$$i_o = i_{L1} + i_{L2} = I_o + i_{o(\omega)} + i_{o(2\omega)} + i_{o(3\omega)} + i_{o(4\omega)} \tag{19}$$

where I_o is the DC component of total output current; $i_{o(\omega)}$, $i_{o(2\omega)}$, $i_{o(3\omega)}$, $i_{o(4\omega)}$ are the first, second, third, and fourth harmonic current components. Detailed expressions of these components can be found in equations (20) – (24).

$$I_o = \frac{I_{\max}V_{\max}}{2V_o} = \frac{P_{ac\_rms}}{V_o} \tag{20}$$

$$i_{o(\omega)} = \left[kC_1 - (1-k)C_2\right]\left(-\frac{\omega V_{\max}V_d}{V_o}\cos(\omega t) + \frac{\omega B V_{\max}}{2V_o}\sin(\omega t + \varphi)\right) \tag{21}$$

$$i_{o(2\omega)} = -\frac{I_{\max}V_{\max}}{2V_o}\cos(2\omega t) - \frac{2\omega B(C_1 + C_2)V_d}{V_o}\cos(2\omega t + \varphi) - \left(k^2C_1 + (1-k)^2C_2\right)\frac{\omega V_{\max}^{\ 2}}{2V_o}\sin(2\omega t) \tag{22}$$

$$i_{o(3\omega)} = \left[kC_1 - (1-k)C_2\right]\left(-\frac{3\omega V_{\max}B}{2V_o}\sin(3\omega t + \varphi)\right) \tag{23}$$

$$i_{o(4\omega)} = -\frac{\omega B^2(C_1 + C_2)}{V_o}\sin(4\omega t + 2\varphi) \tag{24}$$

where P_{ac_rms} is the root-mean-square (RMS) power of the source.

Careful examination of (21) and (23) shows that $i_{o(\omega)}$ and $i_{o(3\omega)}$ will always be zero as long as

$$kC_1 = (1-k)C_2 \tag{25}$$

is satisfied.

Moreover, by equating $i_{o(2\omega)}$ in (22) to zero and combining it with (25), it can be derived that $i_{o(\omega)}$, $i_{o(2\omega)}$ and $i_{o(3\omega)}$ will be eliminated when

$$k = \frac{C_2}{C_1 + C_2} \tag{26}$$

$$B = -\frac{V_{\max}}{4\omega(C_1 + C_2)V_d}\sqrt{{I_{\max}}^2 + (kC_1\omega V_{\max})^2} \tag{27}$$

$$\varphi = \sin^{-1}\frac{I_{\max}}{\sqrt{{I_{\max}}^2 + (kC_1\omega V_{\max})^2}} - \frac{\pi}{2} \tag{28}$$

are complied.

IV. Experimental Validation

A prototype of the buck differential rectifier with the inductor-current waveform control is constructed and tested. Table II gives the rectifier's specifications. LABVIEW is used to calculate and generate the desired inductor current reference signals according to (18) based on the optimal values of k, B, and φ from (26) – (28). Two hysteresis controllers are used to independently control i_{L1} and i_{L2} such that the respective references are tracked. The control blocks are shown in Fig. 5.

TABLE II. SPECIFICATIONS OF BUCK DIFFERENTIAL RECTIFIER

Input voltage V_{ac} (RMS)	110 V
Output voltage V_o	43.6 V
Fundamental frequency f	50 Hz
Switch frequency f_s	around 50 kHz
Inductors (L_1, L_2)	600 uH, 6 A
Capacitors (C_1, C_2)	C_1=C_2=15 uF, 600 V, film cap

With this configuration, the direct AC/DC differential rectifier with mitigated second-harmonic frequency content on the DC side can be realized. It must be emphasized that no electrolytic capacitance is used in the experimental setup. In this experiment (C_1=C_2=15 μF), the adopted parameters are k=0.5, V_d =200 V, and B= –15.27 V and φ= – 0.52.

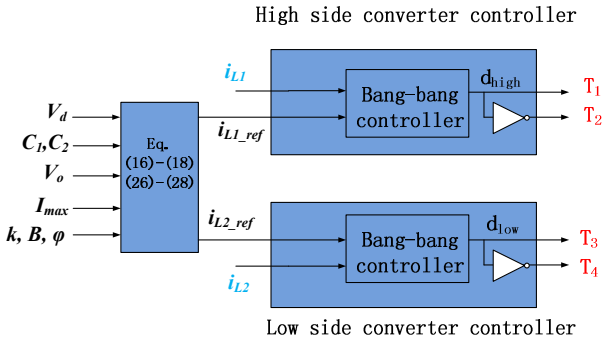

Fig. 5. Control blocks of the differential buck rectifier with current bang-bang controller.

Figs. 6(a)–(d) show the measured voltage and current waveforms of the proposed buck differential rectifier with the proposed inductor-current waveform control operating at 50 W output. A small capacitor (C_o =0.47 μF) is paralleled with the DC load to filter the high frequency switching ripple.

Fig. 6(a) shows the inductor current waveforms of i_{L1} and i_{L2}, and the output current i_o, which is the sum of i_{L1} and i_{L2}. With the proposed inductor-current waveform control, the low-frequency current ripple at the DC output is substantially mitigated. The amplitude of output current ripple is 0.27 A (23 % of average (DC) output current 1.15 A)

Fig. 6(b) shows the voltage waveforms of the input capacitors C_1 and C_2, and the AC input source v_{ac}. Figs. 6(c) and (d) show the waveforms of the line voltage v_{ac} and line current i_{ac}, and the FFT spectrum for the line (i_{ac}) and the output current (i_o), respectively. It is shown that a good power factor with low harmonic contents is achieved. Line current contains negligible (2.69%) 100 Hz (second harmonic) current component and 11.9% of the third harmonic current component. The measured total harmonic distortion (THD) of the input current is 10.45% with a PF of 0.97. These measurements are within the limit of Class C regulation. It should be noted that no front-stage EMI filter is included in the circuit as C_1 and C_2 can adequately provide the high-frequency filtering of i_{ac}. For output current i_o, the 100 Hz content is only 4.2% of the average current.

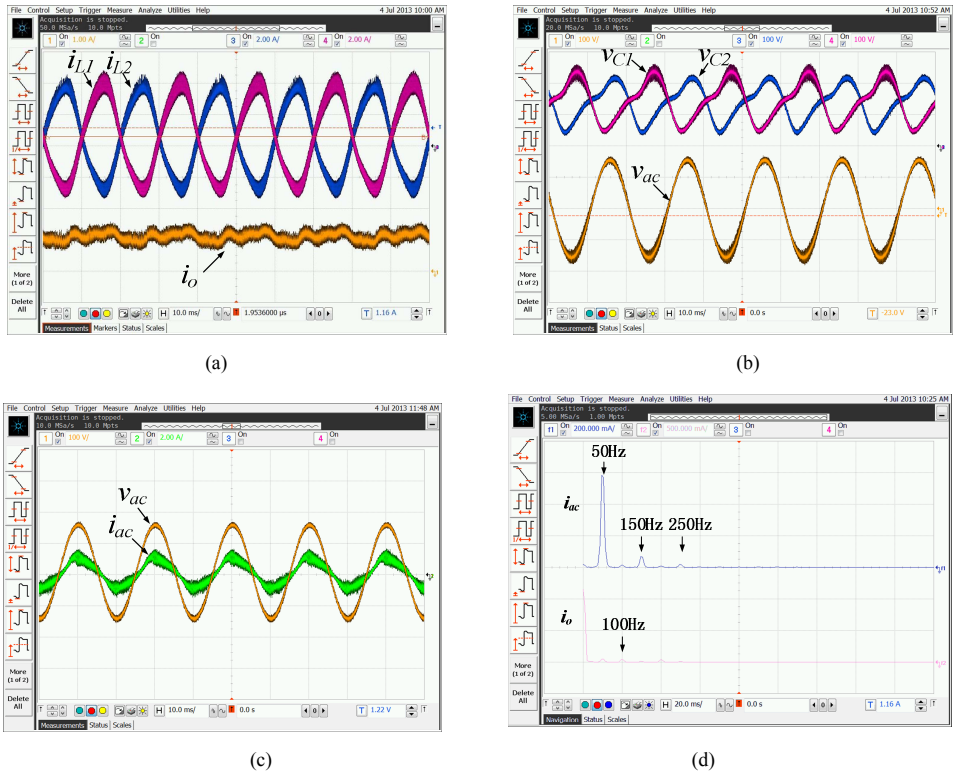

Fig. 6. Experimental results of differential buck converter with operating conditions P_o = 50 W, R_o=39 Ω, C_o=0.47 μF for the dual-cap case of C_1= C_2=15 μF. [(a): inductor currents i_{L1} (pink), i_{L2} (blue) and output current i_o (orange) (b): v_{C1} (pink), v_{C2} (blue), v_{ac} (orange) (c): v_{ac} (orange), i_{ac} (green) (d) FFT analysis results for i_{ac} (orange) and for i_o (green). Scales: i_{L1}, i_{L2}: 2 A/div, i_o: 1 A/div, v_{C1}, v_{C2}, v_{ac}: 100 V/div, i_{ac}: 2 A/div, FFT for i_{ac}: 200 mA/div, FFT for i_o: 500 mA/div

V. CONCLUSIONS

A type of AC/DC differential rectifier system is proposed in this paper for direct rectification applications. The configuration is based on a structure of having two bidirectional DC/DC converters with series-input and parallel-output connections. To complement the feature of this rectifier configuration, inductor-current waveform control is applied to mitigate the second-harmonic current ripple of the DC output, thereby allowing the removal of the electrolytic storage capacitor that is typically required in such systems. Mathematical derivations and analysis are provided in the paper to validate the concept, using the buck differential rectifier as a case study example. Experimental results show that the idea is feasible and workable for this buck rectifier configuration. The idea of the direct AC/DC differential rectifier is extendable to other combination of converters, connected differentially, with or without galvanic isolation, for single phase or multi-phase applications.

REFERENCES

[1] G.-R. Zhu, S.-C. Tan, Y. Chen, and C. K. Tse, "Mitigation of Low-Frequency Current Ripple in Fuel-Cell Inverter Systems Through Waveform Control," *IEEE Trans. Power Electron.*, vol. 28, no. 2, pp. 779–792, Feb. 2013.

[2] B. Wang, X. Ruan, K. Yao, and Ming Xu, "A Method of Reducing the Peak-to-Average Ratio of LED Current for Electrolytic Capacitor-Less AC–DC Drivers," *IEEE Trans. Power Electron.*, vol. 25, no. 3, pp. 592–601, Mar. 2010.

[3] S. Wang, X. Ruan, K. Yao, S.-C. Tan, Y. Yang, and Z. Ye, "A flicker-free electrolytic capacitor-less AC–DC LED driver," *IEEE Trans. Power Electron.*, vol. 27, no. 11, pp. 4540–4548, Nov. 2012.

[4] L. Gu, X. Ruan, M. Xu, and K. Yao, "Means of Eliminating Electrolytic Capacitor in AC/DC Power Supplies for LED Lightings," *IEEE Trans. Power Electron.*, vol. 24, no. 5, pp. 1399–1408, May 2009.

[5] Y. Qin, H. Chung, D. Y. Lin, and S. Y. R. Hui, "Current source ballast for high power lighting emitting diodes without electrolytic capacitor," in *2008 34th Annual Conference of IEEE Industrial Electronics*, 2008, pp. 1968–1973.

[6] W. Chen and S. Hui, "Elimination of an Electrolytic Capacitor in AC/DC Light-Emitting Diode (LED) Driver With High Input Power Factor and Constant Output Current," *IEEE Trans. Power Electron.*, vol. 27, no. 3, pp. 1598–1607, Mar. 2012.

[7] X. Ruan, B. Wang, K. Yao, and S. Wang, "Optimum Injected Current Harmonics to Minimize Peak-to-Average Ratio of LED Current for Electrolytic Capacitor-Less AC–DC Drivers," *IEEE Trans. Power Electron.*, vol. 26, no. 7, pp. 1820–1825, Jul. 2011.

[8] S. Y. (Ron) Hui and Y. X. Qin, "A General Photo-Electro-Thermal Theory for Light Emitting Diode (LED) Systems," *IEEE Trans. Power Electron.*, vol. 24, no. 8, pp. 1967–1976, Aug. 2009.

[9] W. Qi, H. Wang, X. Tan, G. Wang, and K. D. T. Ngo, "A novel active power decoupling single-phase PWM rectifier topology," in *2014 IEEE*

Applied Power Electronics Conference and Exposition - APEC 2014, 2014, pp. 89–95.

[10] P. T. Krein, R. S. Balog, and M. Mirjafari, "Minimum Energy and Capacitance Requirements for Single-Phase Inverters and Rectifiers Using a Ripple Port," *IEEE Trans. Power Electron.*, vol. 27, no. 11, pp. 4690–4698, Nov. 2012.

[11] T. Shimizu, Y. Jin, and G. Kimura, "DC ripple current reduction on a single-phase PWM voltage-source rectifier," *IEEE Trans. Ind. Appl.*, vol. 36, no. 5, pp. 1419–1429, 2000.

[12] K.-H. Chao, P.-T. Cheng, and T. Shimizu, "New control methods for single phase PWM regenerative rectifier with power decoupling function," in *2009 International Conference on Power Electronics and Drive Systems (PEDS)*, 2009, pp. 1091–1096.

[13] H. Li, K. Zhang, H. Zhao, S. Fan, and J. Xiong, "Active Power Decoupling for High-Power Single-Phase PWM Rectifiers," *IEEE Trans. Power Electron.*, vol. 28, no. 3, pp. 1308–1319, Mar. 2013.

[14] S. Y. Hui, S. N. Li, X. H. Tao, W. Chen, and W. M. Ng, "A Novel Passive Offline LED Driver With Long Lifetime," *IEEE Trans. Power Electron.*, vol. 25, no. 10, pp. 2665–2672, Oct. 2010.

[15] W. Chen, S. N. Li, and S. Y. R. Hui, "A comparative study on the circuit topologies for offline passive light-emitting diode (LED) drivers with long lifetime & high efficiency," in *2010 IEEE Energy Conversion Congress and Exposition*, 2010, pp. 724–730.

[16] I. E. Colling and I. Barbi, "Reversible unity power factor step-up/step-down AC-DC converter controlled by sliding mode," *IEEE Trans. Power Electron.*, vol. 16, no. 2, pp. 223–230, Mar. 2001.